An isocyanide probe for heme electronic structure: bis(*tert*-butylisocyanide) complex of diazaporphyrin showing a unique $(d_{xy})^2(d_{xz}, d_{yz})^3$ ground state†

Yoshiki Ohgo,*[ab] Saburo Neya,[c] Hidehiro Uekusa[d] and Mikio Nakamura*[abe]

Received (in Cambridge, UK) 12th July 2006, Accepted 23rd August 2006
First published as an Advance Article on the web 20th September 2006
DOI: 10.1039/b609910f

Isocyanide-bound model hemes always adopt the $(d_{xz}, d_{yz})^4(d_{xy})^1$ ground state, however, we have found that the replacement of porphyrin by diazaporphyrin leads to the formation of an unprecedented low-spin bis(*tert*-butylisocyanide) complex with the $(d_{xy})^2(d_{xz}, d_{yz})^3$ ground state.

The alkyl and aryl isocyanides such as ^{t}BuNC and PhNC are quite unique ligands for iron(III) porphyrinates because their coordination always leads to the formation of low-spin complexes adopting the less common $(d_{xz}, d_{yz})^4(d_{xy})^1$ ground state.[1] In fact, no exception has ever been reported since Simonneaux *et al.* discovered the unusual electronic state of $[Fe(TPP)(^tBuNC)_2]^+$ in 1989.[2,3] Formation of the less common $(d_{xz}, d_{yz})^4(d_{xy})^1$ ground state has been explained in terms of the stabilization of the d_π (d_{xz} and d_{yz}) orbitals caused by the strong interaction with the low-lying p_{π^*} orbital of isocyanide.[1] In this communication, we report that the bis(^{t}BuNC) iron(III) complex adopts the common $(d_{xy})^2(d_{xz}, d_{yz})^3$ ground state when porphyrin is replaced by diazaporphyrin, and that the isocyanide ligand can be a unique probe to elucidate the fine electronic structure of naturally occurring ferric heme proteins.

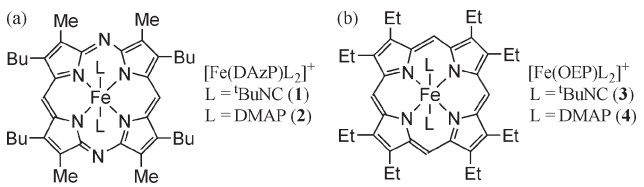

Fig. 1 shows the ^{1}H NMR Curie plots of the α-CH_2 and *meso*-H signals in low-spin $[Fe(DAzP)L_2]^+$ where L's are ^{t}BuNC(**1**) and DMAP(**2**). The Curie plots of the corresponding signals in low-spin $[Fe(OEP)L_2]^+$ where L's are ^{t}BuNC(**3**) and DMAP(**4**) are also given. Fig. 1(a) shows that **1** exhibits the α-CH_2 signal much more downfield than **2**, **3**, and **4**, which indicates that **1** has a fairly large positive spin at the pyrrole β-C.[1] Curie plots of the *meso*-H signals shown in Fig. 1(b) reflect the spin densities at the *meso*-C. For example, the *meso*-H signal of **3** appeared at extremely upfield positions suggesting that the *meso*-C of **3** has a quite large positive spin.

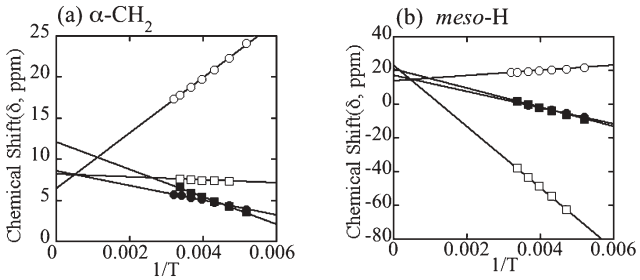

Fig. 1 Curie plots of (a) α-CH_2 and (b) *meso*-H signals of $[Fe(DAzP)L_2]^+$ and $[Fe(OEP)L_2]^+$ taken in CD_2Cl_2 solution, where **1** = ○; **2** = ●; **3** = □ and **4** = ■.

The result indicates that **3** adopts the $(d_{xz}, d_{yz})^4(d_{xy})^1$ ground state; the unpaired electron in the d_{xy} orbital delocalizes to the *meso*-C by the d_{xy}–a_{2u} interaction, and induces the upfield shift of the *meso*-H signal.[1,4] In contrast, the *meso*-H signals of the DMAP complexes (**2** and **4**) appeared slightly more upfield than their diamagnetic positions. The result indicates that the *meso*-C of these complexes has a quite small spin density. This is one of the common features of the low-spin complexes adopting the $(d_{xy})^2(d_{xz}, d_{yz})^3$ ground state.[5] In the case of **1**, the Curie plots showed a peculiar behavior; the *meso*-H signal appeared rather downfield and showed a positive slope. The result suggests that the *meso*-C of **1** could have negative spin, which in turn indicates that **1** does not adopt the $(d_{xz}, d_{yz})^4(d_{xy})^1$ ground state in spite of the coordination of ^{t}BuNC.

For a more quantitative comparison of the spin distribution in the macrocycles of **1–4**, we have determined the spin densities of the peripheral carbon atoms on the basis of the ^{1}H NMR, ^{13}C NMR, and EPR parameters using the Karplus–Frankel equation.†[6,7] Structural data of **1–4**, which are necessary for the spin density analysis, were obtained directly from the X-ray molecular structure in the case of **3** and **4**,[4,8] and from that of analogous $[Fe(DAzP)(4\text{-}CNPy)_2]^+$ in the case of **1** and **2**.[9] The results are given in Table 1. As expected, while **3** has a large spin density, +0.028, at the *meso*-C because of the d_{xy}–a_{2u} interactions, other three complexes, **1**, **2**, and **4**, have more or less negative spin at these carbon atoms. Thus, these three complexes adopt the

[a]*Department of Chemistry, School of Medicine, Toho University, Ota-ku, Tokyo 143-8540, Japan. E-mail: yohgo@med.toho-u.ac.jp; mnakamu@med.toho-u.ac.jp*
[b]*Research Center for Materials with Integrated Properties, Toho University, Funabashi 274-8510, Japan*
[c]*Department of Physical Chemistry, Graduate School of Pharmaceutical Sciences, Chiba University, Chiba 263-8522, Japan*
[d]*Graduate School of Science and Engineering, Tokyo Institute of Technology, Tokyo 152-8551, Japan*
[e]*Division of Chemistry, Graduate School of Science, Toho University, Funabashi 274-8510, Japan*

† Electronic supplementary information (ESI) available: Experimental data, molecular structure of $[Fe(DAzP)(4\text{-}CNPy)_2]ClO_4$, validity of using geometric factors obtained from the molecular structure of analogous $[Fe(DAzP)(4\text{-}CNPy)_2]ClO_4$, ^{1}H NMR, ^{13}C NMR, and EPR data. See DOI: 10.1039/b609910f

Table 1 Chemical shifts (δ) and spin densities (ρ) in **1–4**

	δ/ppm (298 K, CD_2Cl_2)				$\rho_{pyrrole-\beta}$	
Complexes	*meso*-H	α-CH_3	α-CH_2	ρ_{meso-C}	N side	C side
1	19.20	−59.45	−35.40	−0.012	0.016	0.011
2	3.51	−45.80	−21.80	−0.0021	0.010	0.0094
3	−37.71	—	1.70	0.028	0.0047	—
4	1.82	—	−23.50	−0.00083	0.0082	—

$(d_{xy})^2(d_{xz}, d_{yz})^3$ ground state. It should be noted that **1** shows a quite unique spin distribution on the macrocycle. Namely, the *meso*-C's have large negative spin, −0.012, while the pyrrole-β-C's have large positive spin, +0.016 and +0.011. The anomalous spin distribution in the macrocycle of **1** should be ascribed to the presence of low-lying p_{π^*} orbitals of ^{t}BuNC and DAzP.[10] The larger positive spin at the β-C in **1** as compared with those of the DMAP complexes (**2** and **4**) suggests that the singly occupied d_π orbital can more effectively interact with the $3e_g$-like orbital of DAzP due to the smaller energy gap between the two interacting orbitals. This is because the d_π orbital of **1** is stabilized by the low-lying p_{π^*} orbital of ^{t}BuNC, which is absent in the DMAP complexes such as **2** and **4**. Presence of a fairly large negative spin at the *meso*-C's in **1** is more difficult to explain. Cheng and co-workers recently reported on the basis of the DFT calculation that the interaction between doubly occupied a_{2u} orbital with a vacant $d_{x^2-y^2}$ orbital in saddle shaped intermediate-spin $[Fe(OETPP)(THF)_2]^+$ polarizes the paired electrons to leave negative spin in the a_{2u} orbital.[11] In the present case, the interaction of a doubly occupied d_π orbital with a vacant $4e_g$-like orbital could polarize the paired electrons to induce negative spin at the *meso*-C, because the $4e_g$-like orbital has a relatively large coefficient at the *meso*-C. This interaction must be much stronger in **1** than in the corresponding porphyrin complexes with the $(d_{xy})^2(d_{xz}, d_{yz})^3$ ground state because of the short Fe–N bond lengths,[9] nearly planar DAzP structure,[9] and the presence of low-lying $4e_g$-like orbital.[10] It is quite interesting that the replacement of OEP ring by DAzP ring in $[Fe(Por)(^tBuNC)_2]^+$ switches the large positive spin at the *meso*-C to the large negative one.

Meso ^{13}C chemical shift in low-spin iron(III) porphyrinates is a quite good probe to determine the electronic structure.[5,12–14] The $(d_{xz}, d_{yz})^4(d_{xy})^1$ type complexes exhibit the *meso*-C signals extremely downfield by the reasons already mentioned. In contrast, the $(d_{xy})^2(d_{xz}, d_{yz})^3$ type complexes exhibit them more upfield than the corresponding diamagnetic complexes because of the interaction of the singly occupied iron d_π orbital with the porphyrin $3e_g$ orbitals; the *meso* carbons are nodes in the $3e_g$ orbitals. Table 2 shows the *meso* ^{13}C chemical shifts of **1** and **3** together with a wide variety of $[Fe(Por)(^tBuNC)_2]^+$ reported previously. All the complexes except **1** exhibit the *meso*-C signals at extremely downfield positions, 416–997 ppm at 223 K. Although the *meso*-C signals of highly ruffled T^iPrP and T^nPrP complexes were too broad to observe probably due to the short relaxation time, they should appear much lower than 1000 ppm.[5] In sharp contrast, the *meso*-C signal of **1** was observed at 21 ppm, which convinces us that the complex adopts the $(d_{xy})^2(d_{xz}, d_{yz})^3$ ground state.

As is well known, the dipolar shift (δ_{dip}) of the ^{1}H signal is given by eqn (1), where A is a positive constant, $g_\parallel$ and $g_\perp$ are EPR g values, and $(3\cos^2\theta - 1)/r^3$ is a geometric factor.†[1,6] The sign of $(g_\parallel^2 - g_\perp^2)$ is different between two types of low-spin complexes;

Table 2 ^{13}C NMR[a], EPR[b], and IR[c] data of some $[Fe(Por)(^tBuNC)_2]^+$

Por	^{13}C NMR δ_{meso}	EPR g values			ν_{CN}/cm^{-1})	Ground state[d]
DAzP(**1**)	21[e]	3.01	2.05	1.5[e]	2213[e]	d_π
OETPP	416[f]	2.29	2.25	1.92[f]	2195[e]	d_{xy}
OEP(**3**)	491[f]	2.29	2.29	1.86[f]	2193[g]	d_{xy}
OMTPP	979[f]	2.20	2.17	1.95[f]	2193[e]	d_{xy}
TPP	997[f]	2.18	2.18	1.93[f]	2200[g]	d_{xy}
T^nPrP	too broad[f]	2.16	2.16	1.95[f]	2190[e]	d_{xy}
T^iPrP	too broad[f]	2.16	2.16	1.96[f]	2193[e]	d_{xy}

[a] δ ppm, CD_2Cl_2, 223 K. [b] CH_2Cl_2, 4–12 K. [c] CH_2Cl_2, 298 K. [d] d_π and d_{xy} indicate $(d_{xy})^2(d_{xz}, d_{yz})^3$ and $(d_{xz}, d_{yz})^4(d_{xy})^1$, respectively. [e] This work. [f] Ref. 5. [g] Ref. 4.

the $(d_{xy})^2(d_{xz}, d_{yz})^3$ complexes should give positive values while the $(d_{xz}, d_{yz})^4(d_{xy})^1$ complexes should give negative ones.[1]

$$\delta_{dip} = A\left(g_\parallel^2 - g_\perp^2\right)\frac{(3\cos^2\theta - 1)}{r^3}\frac{1}{T} \quad (1)$$

Thus, the slope of the Curie plots could differentiate the two types of low-spin complexes if the contribution of the dipolar shift to the isotropic shift is not negligibly small. Fig. 2 shows the Curie plots of the *tert*-butyl signal of **1** together with those of a wide variety of $[Fe(Por)(^tBuNC)_2]^+$ adopting the $(d_{xz}, d_{yz})^4(d_{xy})^1$ ground state. While the Curie plots of **1** showed a large positive slope, all the other complexes exhibited small negative slopes. Since the geometric factor for the *tert*-butyl protons is positive, the positive slope observed in the Curie plots of **1** suggests that the complex adopts the $(d_{xy})^2(d_{xz}, d_{yz})^3$ ground state.

In order to obtain additional pieces of evidence supporting the $(d_{xy})^2(d_{xz}, d_{yz})^3$ ground state of **1**, we have measured the EPR spectra in frozen CH_2Cl_2 solution at 4–12 K. The EPR spectra shown in Fig. 3 indicate that **1** adopts the $(d_{xy})^2(d_{xz}, d_{yz})^3$ ground state; the low-spin complexes with the $(d_{xz}, d_{yz})^4(d_{xy})^1$ ground state should exhibit the axial type spectra.[1] The g values of **1** were estimated to be 3.01, 2.05, and 1.5 on the basis of the computer simulation of the observed broad signals. In contrast, the EPR spectrum of **2** exhibited clearly resolved signals at g = 2.82, 2.22, and 1.62. Table 2 lists the g values of **1** and **3** together with those of various $[Fe(Por)(^tBuNC)_2]^+$ reported previously.[4] All the complexes except **1** showed the axial type spectra with $g_\perp$ signals at 2.22 ± 0.07. These data again indicate that **1** adopts the $(d_{xy})^2(d_{xz}, d_{yz})^3$ ground state.

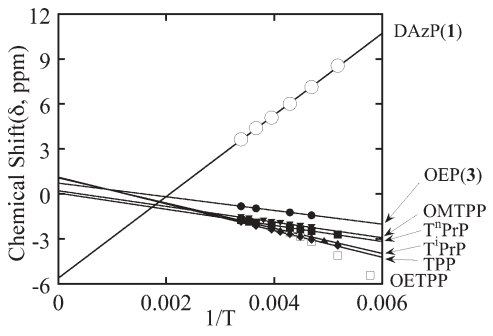

Fig. 2 Curie plots of the *tert*-butyl signals in various $[Fe(Por)(^tBuNC)_2]^+$ taken in CD_2Cl_2 solutions. The porphyrinoids (Por) examined are TPP, T^nPrP, T^iPrP, OMTPP, OETPP, OEP(**3**) and DAzP(**1**, ○). The Curie line for the OETPP complex (□) is omitted because of the large curvature.

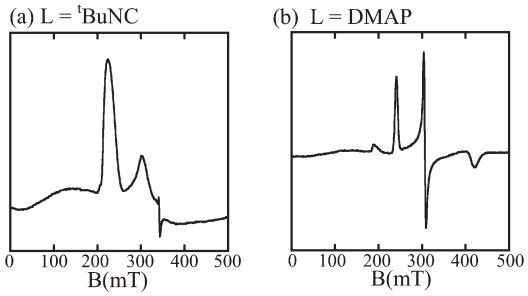

Fig. 3 EPR spectra of (a) **1** and (b) **2** taken in CH_2Cl_2 at 4–12 K.

The difference in electronic ground state should be reflected in the C–N stretching frequencies of the coordinated ^{t}BuNC ligand in the IR spectra. These data are listed in the third column of Table 2. While the complexes with the $(d_{xz}, d_{yz})^4(d_{xy})^1$ ground state exhibited the stretching bands at 2195 $\pm$ 5 cm^{-1}, **1** showed the corresponding band at much higher frequency, 2213 cm^{-1}; the stretching frequency of free ^{t}BuNC is 2139 cm^{-1}. In general, the stretching frequency of isocyanide increases as the σ-bonding is strengthened or π-back-bonding is weakened.[15] Thus, the lower frequencies in the $(d_{xz}, d_{yz})^4(d_{xy})^1$ type complexes can be explained either by the weaker σ-bonding or by the stronger π-back-bonding. Clearly, the latter is the case because the $(d_{xz}, d_{yz})^4(d_{xy})^1$ ground state is caused by the interaction between iron d_π and ligand p_{π^*} orbitals. The higher frequency of **1** can then be explained in terms of the weaker π-back-bonding, which should be ascribed to the DAzP ring having two electron withdrawing nitrogen atoms in the macrocycle; the iron d_π orbital could be involved in the interaction with the $4e_g$-like orbital of DAzP rather than with the p_{π^*} orbital of ^{t}BuNC as mentioned in the previous section.

Isocyanide-bound heme proteins have been used as models for the heme proteins carrying simple diatomic molecules such as O_2, CO, NO, *etc*.[16] The CN stretching frequencies can tell the nature of the heme-ligand σ-bonding as well as π-back-bonding. Surprisingly, **1** showed the CN stretching band at an almost identical position as isocyanide-bound ferric cytochrome $P450_{nor}$ and cytochrome $P450_{cam}$; they are 2214 and 2212 cm^{-1}, respectively.[17] The results indicate that the π-back-bonding in these proteins is rather weak, and that the ferric ions certainly adopt the $(d_{xy})^2(d_{xz}, d_{yz})^3$ ground state. Formation of the $(d_{xy})^2(d_{xz}, d_{yz})^3$ ground state in these isocyanide-bound ferric cytochromes P450 could be explained in terms of the strong σ-donation of the thiolate ligand to the vacant iron d_{z^2} orbital, which results in lengthening the Fe–C bond of the *trans* isocyanide ligand and increasing the C–N stretching frequencies.[18]

In conclusion, we have found for the first time that the low-spin bis(^{t}BuNC) complex (**1**) adopts the $(d_{xy})^2(d_{xz}, d_{yz})^3$ ground state in spite of the presence of axially coordinated ^{t}BuNC ligands on the basis of the ^{1}H NMR, ^{13}C NMR, EPR, and IR spectroscopy, and that **1** exhibits a quite unique spin distribution on the macrocycle as compared with other low-spin complexes with the same electronic ground state. In addition, our finding on the novel $(d_{xy})^2(d_{xz}, d_{yz})^3$ ground state in **1** convinces us that the isocyanide ligand is a quite unique probe to look into the fine electronic structure of heme irons in various heme proteins.

This work was supported by The Reseach Promotion Grant from the Toho University Graduate School of Medicine (no. 05-21 and no. 06-01 to Y. O.), and by The Grant-in-Aid for Scientific Research from the Ministry of Education, Culture, Sports, Science and Technology, Japan (no. 18655025 to Y. O. and no. 16550061 to M. N.). Thanks are due to the Research Center for Molecular-Scale Nanoscience, the Institute for Molecular Science (IMS).

References

1 F. A. Walker, in *The Porphyrin Handbook*, ed. K. M. Kadish, K. M. Smith, R. Guilard, Academic Press, San Diego, 2000, vol. 5, pp. 81–183.
2 Abbreviations: Por: dianion of porphyrin and diazaporphyrin. DAzP, TPP, OEP, T^{n}PrP, T^{i}PrP, OMTPP, and OETPP: dianions of 2,7,12,18-tetrabutyl-3,7,13,17-tetramethyl-5,15-diazaporphyrin, 5,10,15,20-tetraphenylporphyrin, 2,3,7,8,12,13,16,17-octaethylporphyrin, 5,10,15,20-tetrapropylporphyrin, 5,10,15,20-tetraisopropylporphyrin, 2,3,7,8,12,13,16,17-octamethyl-5,10,15,20-tetraphenylporphyrin, and 2,3,7,8,12,13,16,17-octaethyl-5,10,15,20-tetraphenylporphyrin, respectively. ^{t}BuNC, *tert*-butylisocyanide. DMAP: 4-(*N*,*N*-dimethylamino)pyridine. 4-CNPy: 4-cyanopyridine.
3 G. Simonneaux, F. Hindre and M. Le Plouzennec, *Inorg. Chem.*, 1989, **28**, 823–825.
4 F. A. Walker, H. Nasri, I. Turowska-Tyrk, K. Nohanrao, C. T. Watson, N. V. Shokhirev, P. G. Debrunner and W. R. Scheidt, *J. Am. Chem. Soc.*, 1996, **118**, 12109–12118.
5 T. Ikeue, Y. Ohgo, T. Saitoh, T. Yamaguchi and M. Nakamura, *Inorg. Chem.*, 2001, **40**, 3423–3434.
6 The isotropic shift (δ_{iso}) of a carbon in question is given by the Karplus–Frankel equation, $\delta_{iso} - \delta_{dip(MC)} = [(S^C + \Sigma Q_{CX(i)})\rho_C + Q_{X(i)C}\rho_{X(i)}]K + D\rho_C$, where $\delta_{dip(MC)}$ and $\delta_{dip(LC)}$ are the metal-centered, and ligand-centered dipolar shifts, respectively. The spin densities of the carbon (ρ_C) and the neighboring atoms ($\rho_{X(1)}$, $\rho_{X(2)}$, and $\rho_{X(3)}$) were determined by simultaneous solution of the equations. See ref. 7 for more information.
7 (*a*) H. M. Goff, Nuclear Magnetic Resonance of Iron Porphyrins, in *Iron Porphyrins (Physical Bioinorganic Chemistry Series 1)*, ed. A. B. P. Lever and H. B. Gray, Addison-Wesley, Reading, MA, 1983, pp. 237–281.I; (*b*) I. Bertini and C. Luchinat, *Coord. Chem. Rev.*, 1996, **150**, 29–75.
8 K. Safo, G. P. Gupta, F. A. Walker and W. R. Scheidt, *J. Am. Chem. Soc.*, 1991, **113**, 5497–5510.
9 Molecular structure of analogous $[Fe(DAzP)(4\text{-}CNPy)_2]^+$ was determined by X-ray crystallography. A quite planar structure of analogous $[Fe(DAzP)(4\text{-}CNPy)_2]^+$ also supports the electronic structure proposed in this manuscript. Crystal and molecular structural data of analogous $[Fe(DAzP)(4\text{-}CNPy)_2]^+$: $C_{51}H_{60}Cl_3FeN_{10}O_4$, M = 1039.29, triclinic, a = 12.935(4), b = 14.355(6), c = 15.946(6) Å, α = 94.668(8), β = 109.913(9), γ = 109.878(9)°, V = 2552(2) Å^3, T = 80 K, space group P-1 (no. 2), Z = 2, μ(Mo-Kα) = 0.507 mm^{-1}, 35216 reflections measured, 11471 unique (R_{int} = 0.032) which were used in all calculations. $R(F)$ = 0.076 ($I > 2\sigma(I)$), 0.089 (all data), w$R(F^2)$ = 0.24 (($I > 2\sigma(I)$), 0.26 (all data), goodness of fit S = 1.057. CCDC 606379. For crystallographic data in CIF or other electronic format see DOI: 10.1039/b609910f.
10 H. Ogata, T. Fukuda, K. Nakai, Y. Fujimura, S. Neya, P. A. Stuzhin and N. Kobayashi, *Eur. J. Inorg. Chem.*, 2004, 1621–1629.
11 R.-J. Cheng, Y.-K. Wang, P.-Y. Chen, Y.-P. Han and C.-C. Chang, *Chem. Commun.*, 2005, 1312–1314.
12 T. Ikeue, Y. Ohgo, T. Saitoh, M. Nakamura, H. Fujii and M. Yokoyama, *J. Am. Chem. Soc.*, 2000, **122**, 4068–4076.
13 A. Hoshino and M. Nakamura, *Chem. Commun.*, 2005, 915–917.
14 A. Hoshino, Y. Ohgo and M. Nakamura, *Inorg. Chem.*, 2005, **44**, 7333–7344.
15 P. A. Stuzhin, S. I. Vagin and M. Hanack, *Inorg. Chem.*, 1998, **37**, 2655–2662.
16 G. Simonneaux and A. Bondon, in *The Porphyrin Handbook*, ed. K. M. Kadish, K. M. Smith and R. Guilard, Academic Press, San Diego, 2000, vol. 5, pp. 299–322.
17 D.-S. Lee, S.-Y. Park, K. Yamane, E. Obayashi, H. Hori and Y. Shiro, *Biochemistry*, 2001, **40**, 2669–2677.
18 K. M. Vogel, P. M. Kozlowski, M. Z. Zgierski and T. G. Spiro, *Inorg. Chim. Acta*, 2000, **297**, 11–17.

